

The superstructure of the double layer mineral wermlandite $[\text{Mg}_7(\text{Al}_{0.57}, \text{Fe}_{0.43}^{3+})(\text{OH})_{18}]^{2+} \cdot$ $[(\text{Ca}_{0.6}, \text{Mg}_{0.4})(\text{SO}_4)_2(\text{H}_2\text{O})_{12}]^{2-}$

J. Rius

Instituto "Jaime Almera" de Investigaciones Geológicas (C.S.I.C.) c/Alcarria s/n,
Barcelona, Spain

and R. Allmann

Fachbereich Geowissenschaften, Philipps-Universität,
D-3550 Marburg, Federal Republic of Germany

Received: March 19, 1984

Crystal structure / Superstructure / Double layer / Wermlandite

Abstract. The structure of wermlandite, $[\text{Mg}_7(\text{Al}_{0.57}\text{Fe}_{0.43})_2(\text{OH})_{18}]^{2+}$ $[(\text{Ca}_{0.6}, \text{Mg}_{0.4})(\text{SO}_4)_2(\text{H}_2\text{O})_{12}]^{2-}$ has been determined and refined to an R value of 7.2% based on 779 symmetry-independent reflections, of which 224 are unobserved (weighted $R=6.1\%$). The cell dimensions are $a=b=9.303(3)$, $c=22.57(1)$ Å, the space group is $P\bar{3}c1$ with $Z=2$ and $D_x=1.96$ cm⁻³.

The double layer structure of wermlandite is similar to those of pyroaurite and sjögrenite. In these compounds the excess positive charge in the brucite-like main layer is compensated by additional anions in the interlayers. Main and interlayer are connected by O–H...O hydrogen bonds ≥ 2.91 Å. The network of hydrogen bonds could be evaluated.

The reflections of type $h, k=3n, l=2n$ are especially strong and indicate the existence of an eighteenfold trigonal superstructure. The superstructure was solved using partial Fourier and Patterson syntheses.

Introduction

Wermlandite is a highly hydrated sulphate from Långban, Wärmland (Sweden). It occurs as thin pale greenish-gray hexagonal plates upon calcite crystals. The mineral was described by (Moore, 1971), who also did the measurements of the physical and optical properties of wermlandite. Professor Moore kindly provided the crystals for our investigations.

Table 1. Chemical content of wermlandite

	<i>a</i>	<i>b</i>	<i>c</i>	<i>d</i>		
CaO	7.04	16.66	2.44	15.74	3.78	
MnO	0.40		0.11		0.11	0.39
MgO	29.30		14.11		14.28	28.72
Fe ₂ O ₃	7.48	4.21	1.82(Fe)	4.26	7.33	
Al ₂ O ₃	6.30		2.39(Al)		2.42	6.16
CO ₂	2.52	1.11	—	—	—	
SO ₃	—	—	4.00	—	15.98	
H ₂ O	47.13	101.68(H)	83.74	—	37.64	
	100.17				100.00	

a Wet chemical analysis by R. Blix (wt.%)

b Cationic constituents in the unit cell (after Moore (1971)) (20.87 cations)

c As *b*) after subtraction of 1.11 CaCO₃ (\cong 5.73 wt.%) and renorming the number of metal ions to 20. SO₃ and H₂O according to the assumed formula and considering the slight excess of trivalent cations (i. e. 0.26 H₂O replaced by OH)

d wt.% according to *c*)

The structure of wermlandite was assumed to be similar to the double layer structures of pyroaurite and sjögrenite. In these minerals, the excess positive charge in the brucite-like main layer ($a \approx 3.1 \text{ \AA}$) is compensated by additional anions in the highly disordered interlayers. Main and interlayer are connected by O—H...O hydrogen bonds. The crystal structure of wermlandite ($a = 3 \times 3.1 \text{ \AA}$) therefore should consist of alternating layers of two kinds: a brucite-like layer of composition $[\text{Mg}_7(\text{Al}, \text{Fe})_2(\text{OH})_{18}]^{2+}$; and an ordered interlayer of composition $[(\text{Ca}, \text{Mg}) \cdot 2\text{X}^{2-}(\text{H}_2\text{O})_{12}]^{2-}$.

At first the crystal cell contents for wermlandite was assumed as $[\text{Mg}_7(\text{Al}, \text{Fe})_2(\text{OH})_{18}] \cdot [\text{Ca}(\text{CO}_3)_{0.5}(\text{OH})_3 \cdot 15\text{H}_2\text{O}]$, starting from the complete wet chemical analysis performed by R. Blix of the Swedish Natural History Museum in 1938, which is given in (Moore, 1971) and reproduced in Table 1 (column *a*). However the postulated CO₂ content could not be affirmed by our investigations and X²⁻ was established as SO₄²⁻. The reported CO₂ content seems to be caused by a contamination with calcite. The chemical analysis corrected for these two uncertainties is given in Table 1 (column *c, d*).

The trigonal substructure of wermlandite with subperiods $a' = a/3$, $c' = c/2$ was determined by (Allmann, 1976). In the present work, the superstructure determination using partial Fourier and Patterson synthesis shall be reported.

Experimental and crystal data

A lamellar crystal set along the *a* axis was measured on a Philips four-circle diffractometer PW 1100 (MoK α -radiation, graphite monochromator, $\omega/2\theta$ scan). The space group was established as $P\bar{3}c1$ with $a = b = 9.303(3) =$

$3 \times 3.101 \text{ \AA}$ and $c = 22.57(1) = 2 \times 11.285 \text{ \AA}$, $V = 1692 \text{ \AA}^3$, $Z = 2$. The calculated and measured densities are, respectively, $D_x = 1.97$ and $D_m = 1.93 \text{ g cm}^{-3}$ (Moore, 1971), and the crystal dimensions $0.5 \times 0.2 \times 0.07 \text{ mm}^3$. All reflections up to $\theta = 22^\circ$ (and $3h \ 3k \ 2l$ up to $\theta = 30^\circ$) were recorded and the symmetry-related reflections averaged. 555 of the 779 resulting symmetry-independent reflections possess an intensity greater than 2.5σ according to counting statistics. Intensities were corrected for Lorentz and polarization factors. No absorption correction was applied.

The layers with $l = \text{odd}$ ($\approx 47\%$ unobserved reflections) are much weaker than the layers with $l = \text{even}$ ($\approx 19\%$ unobserved reflections). Due to the partial overlapping of the weak reflections ($l = \text{odd}$) by the tails of strong substructure reflections, some of those were found to be stronger than expected. Therefore the intensities of the weak reflections were controlled by means of Weissenberg and Precession photographs and 40 weak reflections were visually corrected. This overlapping was probably caused by the poor quality of the platy crystal, which also was slightly bent.

The mean observed index of refraction for wermlandite, also reported by (Moore, 1971), is $\bar{n}_{\text{obs}} = 1.49$. A Gladstone-Dale calculation using the specific refractive energies in Larsen and Berman (1934) yields $\bar{n}_{\text{calc}} = 1.50$, in very good agreement with the observed value.

To get information about the nature of the anions (CO_3^{2-} or SO_4^{2-}) a small sample of wermlandite was dispersed homogeneously in potassium bromide, pressed into a disc and the infrared spectrum covering the region from 350 cm^{-1} to 1500 cm^{-1} was recorded. After (Moenke, 1962) the infrared-active fundamental vibrations of the SO_4^{2-} -anion are at $600 \dots 680 \text{ cm}^{-1}$ and between $1050 \dots 1200 \text{ cm}^{-1}$, while the CO_3^{2-} -anion exhibits a strong absorption band in the region $1425 - 1450 \text{ cm}^{-1}$ and a medium strong band between 860 and 887 cm^{-1} . Wermlandite shows two absorption bands at 650 cm^{-1} and at 1105 cm^{-1} (see Fig. 1) significant for SO_4^{2-} , whereas the CO_3^{2-} bands are missing. As Brindley and Kikkawa (1979) report for similar structures an IR-band for CO_3^{2-} near 1350 cm^{-1} , the existence of carbonate ions cannot be completely excluded, but the X-ray structure determination proved SO_4^{2-} to be the main ion, even though the structure determination started with CO_3^{2-} as the interlayer anion. (Compare also the IR spectra of hydrohonesite; Nickel and Wildman, 1981).

Superstructure determination

Allmann (1976), still assuming a carbonate interlayer, showed the subperiods $a' = a/3$, $c' = c/2$ to be determined by the brucite-like $\text{Me}(\text{OH})_2$ -mainlayer in wermlandite. Every subcell includes a metallic cation Me, two OH^- -groups and $1/9 \text{ Ca}^{2+}$. The coordinates of these referred to a' , b' , c' are Me: $(0, 0, 0)$; OH^- : $(1/3, 2/3, -0.090)$ and $1/9 \text{ Ca}^{2+}$: $(0, 0, 1/2)$. The value of $a' = 3.10 \text{ \AA}$ of the brucite-like layer in wermlandite is slightly shorter than the

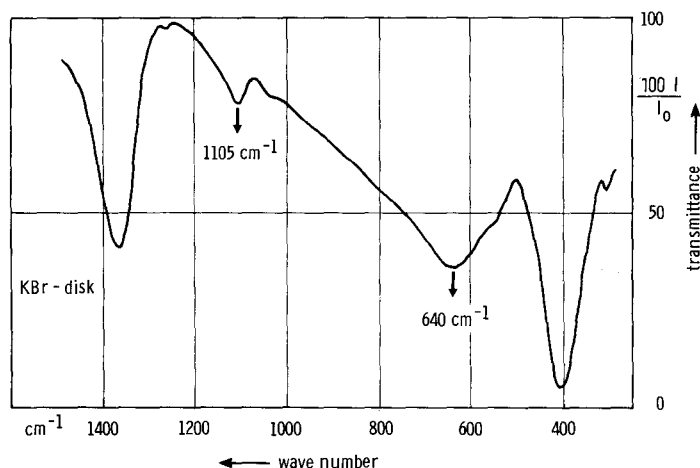


Fig. 1. IR spectrum of wermlandite (pressed in KBr)

Table 2. Steps in the determination of the superstructure. The designations e(9) (e = equivalent) and k(2) (k = klassengleich, i.e. same crystal class) correspond to those of Bärnighausen (1975) and indicate the type and order of symmetry reduction

	$P\bar{3}m1$ (subcell)	
	$h, k = 3n, l = 2n$	
	148 reflections (1 unobs.)	
$3a'3b'$	↓	e(9)
	$P\bar{3}m1$ ("intermediate cell")	
	$hk, l = 2n$	
	510 reflections (98 unobs.)	
$2c'$	↓	k(2)
	$P\bar{3}c1$ (supercell)	
	hkl	
	779 reflections (224 unobs.)	

value $a = 3.14 \text{ \AA}$ for brucite, but like $a = 3.07 \text{ \AA}$ for the $\text{Mg}_3\text{Al}(\text{OH})_8$ -layer of hydroxalcite and $a = 3.11 \text{ \AA}$ for the $\text{Mg}_3\text{Fe}(\text{OH})_8$ -layer of pyroaurite (Allmann, 1970). This difference evidences a partial substitution of Mg^{2+} by smaller cations like Al^{3+} and Fe^{3+} in the main layer of wermlandite.

The first step in the solution of the superstructure was the determination of the "intermediate structure", i.e. those atoms with period (abc') (Table 2). The symmetry reduction of index 9 involved in this step ($a'b'c'$) \rightarrow (abc') is partially due to the presence of the "Ca²⁺" at (0, 0, 1/2) and to the partial ordering of the Al^{3+} and Fe^{3+} at the Me-sites (2/3, 1/3, 0) and (1/3, 2/3, 0) referred to (abc'). This ordering was concluded from the heights of the (Ca – Me) interatomic peaks in a normal Patterson synthesis; consequently, these Me-sites were occupied according to the $\text{Al}^{3+} : \text{Fe}^{3+}$ ratio given by the chemical analysis i.e. $\text{Al}_{0.57}^{3+}, \text{Fe}_{0.43}^{3+}$. These Me-sites with higher electron

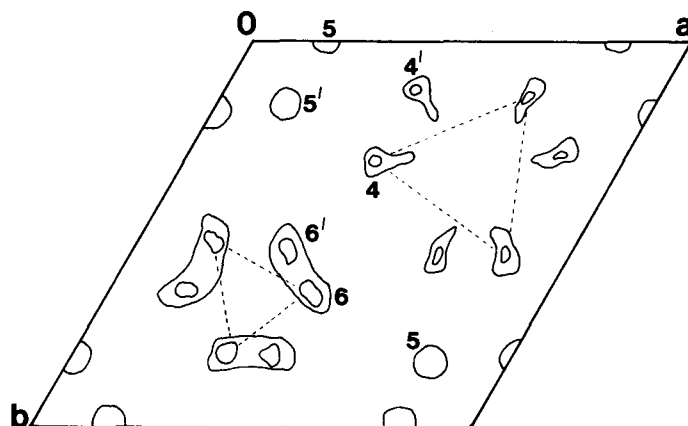


Fig. 2. Section of partial Fourier synthesis $\bar{\rho}(\vec{x})$ in $z \sim 0.08$ (and 0.58). (Reflections with $l = 2n$ only, phases calculated with main layer atoms and Ca). Compare Fig. 4 (because of interchanged axes both figures fit directly)

density will produce additional weak contributions to the reflections of type $h - k = 3n, l = 2n$.

A subsequent partial electron density synthesis $\bar{\rho}(\vec{x})$ (with $l = 2n$ only) yielded the so-called superposition structure i.e. the averaged subcell with respect to c' . Since the symmetry reduction associated with the transition for the "intermediate structure" to the superstructure has index 2, each atom not pertaining to the "intermediate structure" i.e. those with period (abc) , will appear in the $\bar{\rho}(\vec{x})$ -synthesis with half its weight at the true position and at a second position shifted to it by $c/2$, whereas the atoms forming the "intermediate structure" appear with correct weights because they are connected by a pseudo translation of $c/2$. The $\bar{\rho}(\vec{x})$ -synthesis clearly revealed the positions of the remaining atoms of the intermediate structure i.e. S at $(1/3, 2/3, 0.306)$ and O(7) at $(1/3, 2/3, -0.243)$. This synthesis also supplied 3 sets of peaks with half weight at heights $z' = 0.31$ to 0.33 as shown in Figure 2. The O(5) and O(5') peaks correspond to the neighbouring atoms of "Ca²⁺" and are water molecules. The averaged (i.e. doubled) coordination polyhedron of "Ca²⁺" with respect to c' is a regular hexagonal prism. The O(6) and O(6') atoms correspond to the base of the SO₄⁻-group (found distances: S-O(6) = 1.48 Å; S-O(7) = 1.43 Å).

The symmetries of the superstructure and the "intermediate structure" are $P\bar{3}c1$ and $P\bar{3}m1$ respectively. The two possible ways of placing the intermediate structure atoms in the superstructure are:

model (I)	Me(1) at 2(a)	(001/4, 003/4)
	Me(2) and Me(2')	at 6(f) with $x \approx 1/3$ or $\approx 2/3$
	Me(3) at 4(d)	with $z \approx 1/4$
	"Ca ²⁺ " at 2(b)	(000, 001/2)

The Me(3)-sites are those with higher electron density. The symmetry of the site 2(b), i.e. $\bar{3}$, as well as the distribution of O(5) and O(5') in $\bar{\rho}(\vec{x})$ force the coordination polyhedron of "Ca²⁺" to be an octahedron compressed along the [001] direction.

model (II)	Me(1) at 2(b)	(000, 001/2)
	Me(2) at 12(g)	with $x \approx 1/3$, $z \approx 0$ and $y \approx 0$
	Me(3) at 4(d)	with $z \approx 0$
	"Ca ²⁺ " at 2(a)	(001/4, 003/4)

The 18 Me-sites are arranged at $z=0$ and $1/2$ instead of $z=1/4$ and $3/4$ as in the preceding case. The coordination polyhedron for "Ca²⁺" is a trigonal prism now (symmetry for the 2(a) site = $\bar{3}2$). Since the hydroxyl groups are on the c -glide planes, they are connected by a pseudo translation of $c/2$ in both models.

The complementary structure is defined as the difference between the superstructure and the superposition structure i.e. $\delta(\vec{x}) = \rho(\vec{x}) - \bar{\rho}(\vec{x})$ (Takéuchi, 1972), and contains positive and negative peaks. Ignoring the negative ones, the structure so obtained will show the positions of the atoms with period (abc) e.g. with half their weights in the case of wermlandite. Unfortunately, $\delta(\vec{x})$ cannot be calculated before $\rho(\vec{x})$ is known. One way to obtain information about $\delta(\vec{x})$ is the use of the Patterson function of the complementary structure alone. For example, this partial Patterson synthesis $\delta p(\vec{u})$ was used to determine the coordination polyhedron of "Ca²⁺", i.e. the correct model, in the case of wermlandite using those reflections for which $l = \text{odd}$. It may be shown that in the case of the octahedron (model I) a strong negative peak has to appear at ($u=0$ $v=0$ $w=0.14$), whereas in the case of the trigonal prism (s. model II) this peak must be positive. The δP -synthesis revealed the existence of a strong minimum at this point; consequently, only model (I) was considered. All the four possibilities of placing O(4) or O(4'), O(6) or O(6') with O(5) fixed were refined and the correct one was found.

Refinement

Assuming Ca²⁺ as interlayer cation the structure was refined (X-ray system, 1970) to an R -value of 11.6%. Only the isotropic temperature factor of "Ca²⁺" was abnormally high (5.0 Å²). The integration of the electron density on a F_0 -synthesis yielded 16.3 electrons for S and 15.0 for "Ca²⁺". All the H-atoms were localized by a Δ -Fourier syntheses. The H-atoms of the main layer clearly showed up 0.94 Å directly above the corresponding oxygens. The H-atoms with fixed isotropic temperature factors were introduced in the next cycle ($R=8.8\%$).

The partial replacement of Ca²⁺ by Mg²⁺ at site (0, 0, 0) was deduced by two different methods: According to the corrected chemical analysis

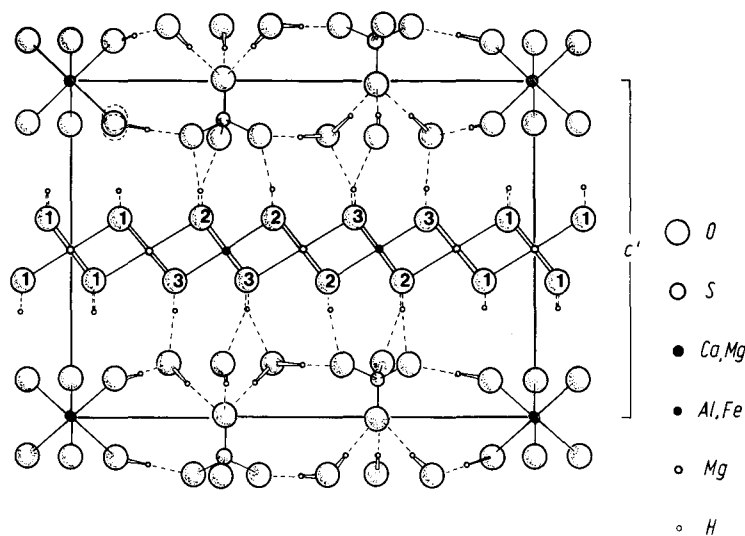


Fig. 3. Wermlandite crystal structure projected onto (110). (An about two atoms wide strip along $x, y = 1, 0; 2/3, 1/3; 1/3, 2/3; 0, 1$)

(Table 1) and assuming all the trivalent cations to be in the main layer, this layer will have an excess of 0.33 Mg^{2+} , so that the probable occupancy will be $\text{Ca}_{0.67}^{2+}, \text{Mg}_{0.33}^{2+}$. The second method is based on the comparison of the observed mean (Ca, Mg)–O(5) bond distances to the tabulated Mg–O and Ca–O bond distances, and gives an occupancy of $\text{Ca}_{0.4}, \text{Mg}_{0.6}$. Due to the influence of the high temperature factors of “ Ca^{2+} ” and O(5) on the mean bond distance, this second occupancy is less reliable, and therefore the compromise occupancy $\text{Ca}_{0.6}, \text{Mg}_{0.4}$ was introduced in the next cycle.

The R -value decreased to 7.2% (weighted $R = 6.1\%$). The following weighting scheme was applied: $w = (0.75 + 0.018 F_o + 21.3/F_o)^{-2}$. The final atomic parameters are listed in Table 3.

Discussion

The crystal structure of wermlandite has been determined to consist of alternating layers of two kinds: a brucite-like layer of composition $[\text{Mg}_7(\text{Al}_{0.57}, \text{Fe}_{0.43}^{3+})_2(\text{OH})_{18}]^{2+}$; and an ordered interlayer of composition $[(\text{Ca}_{0.6}, \text{Mg}_{0.4})(\text{SO}_4)_2(\text{H}_2\text{O})_{12}]^{2-}$. The final averaged Me–OH bond distances for the different Me-sites of the main layer are: Me(1)–OH = 2.066(6), Me(2)–OH = 2.085(8), Me(2')–OH = 2.062(8), and Me(3)–OH = 2.000(7) Å. The comparison of these distances with those calculated for octahedrally coordinated cations (Shannon and Prewitt, 1969), i.e. Mg^{2+} –O = 2.12, Al^{3+} –O = 1.935 and Fe^{3+} –O = 2.045 Å, indicates a possible partial exchange

Table 3. Final atomic parameters of wermlandite ($R=7.2\%$). Values with * were not refined. The anisotropic B_{ik} belong to the expression $\exp(-1/4(h^2a^2B_{11} + \dots + 2klb^*c^*B_{23}))$. B_{ik} in \AA^2

Atom	$x(\sigma)$	$y(\sigma)$	$z(\sigma)$	B/B_{11}	B_{22}	B_{33}	B_{12}	B_{13}	B_{23}
Mg(1)	0	0	1/4	0.67	B_{11}	0.79	$B_{11}/2$	0	0
Mg(2)	0.3319(5)	0	1/4	0.68	0.82	1.00	$B_{22}/2$	$B_{23}/2$	0.10
Mg(3)	0.6672(5)	0	1/4	0.87	0.65	0.86	$B_{22}/2$	$B_{23}/2$	-0.09
(Al, Fe)	2/3	1/3	0.2479(1)	1.18	B_{11}	1.81	$B_{11}/2$	0	0
(Ca, Mg)	0	0	0	3.79	B_{11}	5.11	$B_{11}/2$	0	0
S	1/3	2/3	0.0571(2)	2.60	B_{11}	2.59	$B_{11}/2$	0	0
OH(1)	0.1138(1)	0.2227(5)	0.2046(1)	2.24	1.67	1.06	1.49	0.17	0.02
OH(2)	0.1182(5)	0.5597(8)	0.2062(1)	1.53	1.58	1.32	0.82	0.20	-0.01
OH(3)	0.4504(5)	0.2272(8)	0.2041(1)	1.67	1.57	0.63	0.64	-0.13	-0.53
H ₂ O(4)	0.4262(11)	0.3101(9)	0.0815(3)	5.07	3.71	4.46	1.80	0.13	-0.63
0.4H ₂ O(51)	0.184(2)	-0.013(2)	0.050(1)	2.88	1.31	9.80	0.11	-1.49	-1.52
0.6H ₂ O(52)	0.183(2)	-0.008(2)	0.066(1)	4.14	3.17	6.91	2.23	0.53	-1.32
O(6)	0.4632(11)	0.6373(12)	0.0800(3)	6.12	8.93	5.38	4.46	-0.15	0.79
O(7)	2/3	1/3	0.0049(4)	2.66	B_{11}	2.83	$B_{11}/2$	0	0
H(1)	0.119(11)	0.209(9)	0.163(3)	2.0*					
H(2)	0.144(10)	0.564(10)	0.165(2)	1.1*					
H(3)	0.452(9)	0.234(11)	0.166(3)	1.1*					
H(41)	0.442(20)	0.405(17)	0.090(7)	10*					
H(42)	0.507(15)	0.318(20)	0.055(5)	10*					
H(51)	0.251(16)	-0.087(16)	0.061(6)	8*					
H(52)	0.265(18)	0.092(19)	0.066(6)	10*					

The H₂O(5) position is split, but not so the corresponding H-positions H(51) and H(52)

Table 4. Bond lengths (Å, upper value) and bond valences (v.u., lower value) in wermlandite, $[\text{Mg}_7(\text{Al}_{0.57}, \text{Fe}_{0.43})_2(\text{OH})_{18}]^{2+} \cdot [(\text{Ca}_{0.6}, \text{Mg}_{0.4})(\text{SO}_4)_2(\text{H}_2\text{O})_{12}]^{2-}$

Anion	Cation						\sum_c	charge compensation in H-bridges	$\Sigma v_{\text{corr.}}$
	1/6 Mg(1)	1/2 Mg(2)	1/2 Mg(3)	1/3 (Al, Fe)	1/6 (Ca, Mg)	1/3 S			
OH(1)	2.066(5) 0.33	2.069(7) 0.35	2.040(7) 0.35				1.03		1.03
OH(2)		2.084(7) 0.33	2.070(7) 0.33	2.020(6) 0.49			1.15	-0.12	1.03
OH(3)		2.104(7) 0.32	2.076(7) 0.32	2.003(6) 0.51			1.15	-0.12	1.03
H ₂ O(4)							0.00	-0.14 - 0.18 + 0.12 + 0.19	-0.01
H ₂ O(5)					2.20* 0.33		0.33	-0.19 - 0.16	-0.02
O(6)						1.461(10) 1.44	1.44	+0.12 + 0.14 + 0.16	1.86
1/30(7)						1.400(10) 1.70	1.70	+0.18(3 ×)	2.24
L	2.066	2.086	2.062	2.012	(2.290) (2.105)	1.446	hydrogen bond lengths		∗ at H
L(1)	1.604	1.623	1.599	1.746	(1.837) (1.642)	1.593	OH(2) ... O(6) = 2.92(1) Å		172°
2k	0.97	0.97	0.97	0.88	0.95	0.84	OH(3) ... H ₂ O(4) = 2.91(1)		159
\sum_a	1.98	2.00	2.00	3.00	1.98	6.02	H ₂ O(5) ... H ₂ O(4) = 2.75(2)		177
							H ₂ O(5) ... O(6) = 2.81(2)		167
							H ₂ O(4) ... O(6) = 2.89(1)		160
							H ₂ O(4) ... O(7) = 2.75(1)		179
*) Ca - H ₂ O(52) = 2.290(18) Å				(no H-bond: OH(1) ... H ₂ O(5) = 3.42)					
Mg - H ₂ O(51) = 2.105(18)				∗ at H(1): 151°					

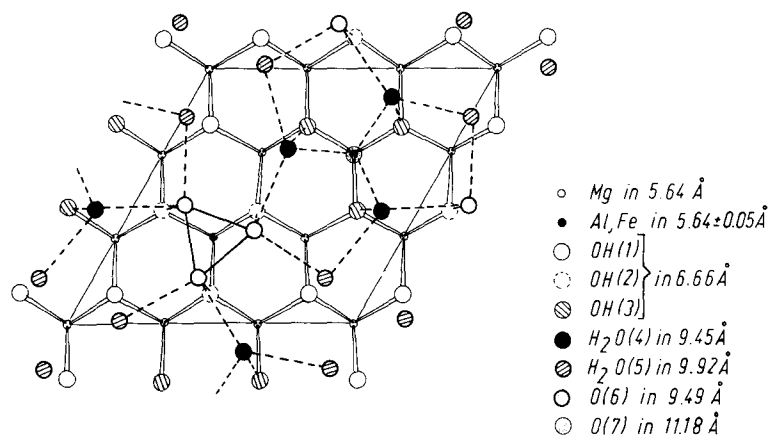


Fig. 4. Network of hydrogen bonds between main layer (OH at $z=0.295$) and interlayer (H_2O and O at $z\sim 0.42$) in wermlandite. y -axis to the right, x -axis down. The triangle at $x, y=2/3, 1/3$ is the base of an SO_4 -group

Table 5. Coordination of $H_2O(4)$ and $H_2O(5)$ in wermlandite. ($\sigma(O-O)=0.01-0.02 \text{ \AA}$). \rightarrow : direction of H-bond

Atoms	distance	angle at the central atom	
$H_2O(4) \leftarrow H_2O(5)$	2.75 Å	$H_2O(5)-O(7)$	100°
$\rightarrow O(7)$	2.75	$H_2O(5)-O(6)$	137
$\rightarrow O(6)$	2.89	$H_2O(5)-OH(3)$	90
$\leftarrow OH(3)$	2.91	$O(7)-O(6)$	104
		$O(7)-OH(3)$	117
		$O(6)-OH(3)$	108
		average(6)	109
$H_2O(5) - Ca, Mg$	2.20	$Ca, Mg-H_2O(4)$	108
$\rightarrow H_2O(4)$	2.75	$Ca, Mg-O(6)$	143
$\rightarrow O(6)'$	2.81	$H_2O(4)-O(6)$	100
$\dots O(5)'$	3.04	average(3)	177*
$\dots OH(1)$	3.42		

* Nearly planar coordination indicates sp^2 -state for $H_2O(5)$ $O(6)'$: $1-y, x-y, z$, $O(5)'$: $-y, x-y, z$

between divalent and trivalent cations e.g. somewhat Mg^{2+} at Me(3) and some Fe^{3+} , Al^{3+} at Me(1), Me(2) and Me(2'). This model was refined, but the R -value did not decrease. There is still another way to explain these differences, i.e. all the Fe^{3+} remains at Me(3) and somewhat Mg^{2+} is substituted by Al^{3+} . Since Al^{3+} and Mg^{2+} are indistinguishable by X-ray diffraction methods, this second model could not be confirmed.

Most of the charge compensation between main layer and interlayer is achieved by the H-bridges $\text{OH}(2) - \text{O}(6) = 2.92 \text{ \AA}$ and $\text{OH}(3) - \text{H}_2\text{O}(4) = 2.91 \text{ \AA}$. However, the $\text{OH}(1) - \text{H}_2\text{O}(5)$ interaction is rather weak ($\text{OH}(1) - \text{H}_2\text{O}(5) = 3.41 \text{ \AA}$), because the $\text{OH}(1)$ -ion is bound to divalent cations only i.e. to the Mg at Me(1), Me(2) and Me(2').

Unlike similar double layer compounds (Allmann, 1970), the interlayer of wermlandite is almost completely ordered. Only the (0, 0, 0) site is statistically occupied according to $\text{Ca}:\text{Mg} = 0.6:0.4$. This fact together with the elongated shape of the thermal vibration ellipsoid of $\text{H}_2\text{O}(6)$ indicated the convenience of splitting it up into 0.6 $\text{H}_2\text{O}(51)$ and 0.4 $\text{H}_2\text{O}(52)$ ($\text{H}_2\text{O}(51) \dots \text{H}_2\text{O}(52) = 0.36 \text{ \AA}$). The octahedron formed by $\text{H}_2\text{O}(5)$ around (Ca, Mg) is slightly compressed along [001] ($\text{H}_2\text{O}(51) \dots \text{H}_2\text{O}(51) = 2.88$ and 3.07 \AA ; $\text{H}_2\text{O}(52) \dots \text{H}_2\text{O}(52) = 3.01$ and 3.45 \AA). In order to assign bond valences v to the experimentally determined interatomic distances, the method proposed by (Allmann, 1975) has been used. The balance of the electrostatic valences is given in Table 4. $\text{H}_2\text{O}(5)$ is tightly bound to (Ca, Mg) (0.33 v.u.) and shows a sp_2 -hybridization. $\text{H}_2\text{O}(4)$ exhibits a sp_3 -hybridization. Each $\text{H}_2\text{O}(4)$ accepts one H-bond from $\text{H}_2\text{O}(5)$ and one from $\text{OH}(3)$ i.e. $0.19 + 0.12 = 0.31$ v.u.

The SO_4 -groups are formed by two symmetry independent oxygens O(6) and O(7) ($\text{O}(6) \dots \text{O}(6) = 2.37 \text{ \AA}$; $\text{O}(6) \dots \text{O}(7) = 2.36 \text{ \AA}$). Each O(7) acts as acceptor of three H-bonds from $\text{H}_2\text{O}(4)$, i.e. $3 \times 0.18 = 0.54$ v.u., and each O(6) accepts one from $\text{OH}(2)$, one from $\text{H}_2\text{O}(5)$ and one from $\text{H}_2\text{O}(4)$ i.e. $0.12 + 0.16 + 0.14 = 0.42$ v.u. The total charge compensated by the sulphate group is thus $3 \times 0.42 + 0.54 = 1.80$ v.u. The theoretical value is 2.00 v.u. This difference may be explained by the fact, that the positions of O(7) and S slightly moved together from their ideal positions during the refinement. To obtain a better balance of the electrostatic charges, the positions of O(7) and S should be shifted by approx. 0.04 and 0.02 \AA in opposite directions.

This 11 \AA -mineral with an ordered sulphate and cation bearing interlayer may be a model for related minerals, for which the superstructure is not yet known, but which are easily transformed to pyroaurite-like 8 \AA -structures by anion-exchange, e.g. in an 1M Na_2CO_3 -solution. Such 11 \AA -minerals are: carrboydite ($a = 3.018$, $c = 3 \times 10.53 \text{ \AA}$, Nickel and Clarke, 1976) hydrohonesite ($a = 3.084$, $c = 3 \times 11.13 \text{ \AA}$, Bish and Livingstone, 1981) motukoreaita ($a = 3 \times 3.112$, $c = 4 \times 11.18 \text{ \AA}$, Rodgers et al., 1977; or $a = 3.062$, $c = 3 \times 11.17 \text{ \AA}$, Brindley, 1979) mountkeithite ($a = \sqrt{12} \times 3.088$, $c = 2 \times 11.272 \text{ \AA}$, Hudson and Bussel, 1981) sulphate-takovite ($a = 3(?) \times 3.024$, $c = 3 \times 10.83 \text{ \AA}$, Bish, 1978) and woodwardite ($a' = 3.07(?)$, $c' = 10.9 \text{ \AA}$, Nickel, 1976).

The 11 \AA -structure may partly be destroyed just by grinding. Similarly dehydration by relative humidities $< 50\%$ leads e.g. for sulphate-takovite to an 8.9 \AA basal spacing (Bish, 1978). Therefore some of the reported powder patterns probably belong to mixtures of differently hydrated or anion-

exchanged specimens e. g. the powder lines for wermlandite, as reported by Moore (1971), at 7.98 (100), 3.89 (202), 3.324 (208), 2.032 (?), 1.668 (414), and 1.512 Å (?) do not fit in with the single crystal data or at least have a too strong intensity¹.

Acknowledgements. We thank Professor Paul B. Moore for donating the wermlandite sample. One of the authors (Rius, J.) wish to thank the DAAD (Deutsches Akademisches Austauschdienst) for financial support. This research was part of Dr. Rius' thesis (Marburg, 1980).

References

- Allmann, R.: Doppelschichtstrukturen mit brucitähnlichen Schichtionen $(\text{Me(II)}_{1-x}\text{Me(III)}_x(\text{OH})_{\frac{1}{2}})^+$. *Chimia* **24**, 99–108 (1970)
- Allmann, R.: Beziehungen zwischen Bindungslängen und Bindungsstärken in Oxidstrukturen. *Monatsh. Chem.* **106**, 779–793 (1975)
- Allmann, R.: Neues über Doppelschichtstrukturen. *Fortschr. Mineral.* **54**, Beiheft 1, S. 3 (1976)
- Bärninghausen, H.: Group-subgroup relations between space groups as an ordering principle in crystal chemistry: The "family tree" of perovskite-like structures. *Acta Crystallogr.* **31**, abstract 0.1.1–9 Amsterdam (1975)
- Bish, D. L.: Anion-exchange in takovite. *Bull. Bur. Rech. Geol. Minières (Fr) Sect. 2*, **3**, 293–301 (1978)
- Bish, D. L., Livingstone, A.: The crystal chemistry and paragenesis of honessite and hydrohonessite. *Mineral. Mag.* **44**, 339–343 (1981)
- Brindley, G. W.: Motukoreaite – additional data and comparison with related minerals. *Mineral. Mag.* **43**, 337–340 (1979)
- Brindley, G. W., Kikkawa, S.: A crystal-chemical study of Mg, Al and Ni, Al hydroxy-perchlorates and hydroxy-carbonates. *Am. Mineral.* **64**, 836–843 (1979)
- Hudson, D. R., Bussel, M.: Mountkeithite, a new pyroauriter-related mineral with an interlayer containing exchangeable MgSO_4 . *Mineral. Mag.* **44**, 345–350 (1981)
- Larsen, E. S., Berman, H.: The microscopic determination of nonopaque minerals. *U.S. Geol. Surv. Bull.* **848**, 31 (1934)
- Moenke, H.: *Mineralspektren* (Ultrarotabsorptions-Spektren... im Spektralbereich 400–4000 cm^{-1}). Akademie-Verlag, Berlin (1962)
- Moore, P.: Wermlandite, a new mineral from Långban, Sweden. *Lithos* **4**, 213–217 (1971)
- Nickel, E. H.: New data on woodwardite. *Mineral. Mag.* **40**, 644–647 (1976)
- Nickel, E. H., Clarke, R. M.: Carrboydite, a hydrated sulfate of nickel and aluminium. *Am. Mineral.* **61**, 366–372 (1976)
- Nickel, E. H., Wildman, J. E.: Hydrohonessite – a new hydrated Ni–Fe hydroxy-sulphate mineral. *Mineral. Mag.* **44**, 333–337 (1981)
- Rodgers, K. A., Chisholm, J. E., Davis, R. J., Nelson, C. S.: Motukoreaite, a new hydrated carbonate, sulphate and hydroxide of Mg and Al from Auckland, New Zealand, *Mineral. Mag.* **41**, 389–390 and M21–23 (1977)
- Shannon, R. D., Prewitt, C. T.: Effective ionic radii in oxides and fluorides. *Acta Crystallogr.* **B25**, 925–946 (1969), revised in *Acta Crystallogr.* **A32**, 751–767 (1976)
- Takéuchi, Y.: The investigation of superstructures by means of partial Patterson functions. *Z. Kristallogr.* **135**, 120–136 (1972)

¹ Additional material to this paper can be ordered from the Fachinformationszentrum Energie-Physik-Mathematik, D-7514 Eggenstein-Leopoldshafen 2, FRG. Please quote reference no. 50737, the names of the authors and the title of the paper.